Resolving the Coupled Effects of Hydrodynamics and DLVO Forces on Colloid Attachment in Porous Media

Saeed Torkzaban,[†] Scott A. Bradford,*[,‡] and Sharon L. Walker[†]

Department of Chemical and Environmental Engineering, University of California, Riverside, Riverside, California 92521, and U.S. Salinity Laboratory, Agricultural Research Service (ARS), U.S. Department of Agriculture (USDA), Riverside, California 92507

Received April 5, 2007. In Final Form: June 16, 2007

Transport of colloidal particles in porous media is governed by the rate at which the colloids strike and stick to collector surfaces. Classic filtration theory has considered the influence of system hydrodynamics on determining the rate at which colloids strike collector surfaces, but has neglected the influence of hydrodynamic forces in the calculation of the collision efficiency. Computational simulations based on the sphere-in-cell model were conducted that considered the influence of hydrodynamic and Derjaguin−Landau−Verwey−Overbeek (DLVO) forces on colloid attachment to collectors of various shape and size. Our analysis indicated that hydrodynamic and DLVO forces and collector shape and size significantly influenced the colloid collision efficiency. Colloid attachment was only possible on regions of the collector where the torque from hydrodynamic shear acting on colloids adjacent to collector surfaces was less than the adhesive (DLVO) torque that resists detachment. The fraction of the collector surface area on which attachment was possible increased with solution ionic strength, collector size, and decreasing flow velocity. Simulations demonstrated that quantitative evaluation of colloid transport through porous media will require nontraditional approaches that account for hydrodynamic and DLVO forces as well as collector shape and size.

1. Introduction

Accurate prediction of the transport and fate of colloidal particles in saturated porous media is of practical interest for many environmental applications, including deep-bed filtration in water and wastewater treatment, transport of colloids and colloid-associated pollutants in groundwater, and natural filtration of microorganisms such as bacteria, viruses, and protozoa.[1−11] Colloid deposition under saturated conditions is commonly described by colloid filtration theory (CFT), originally developed by Yao et al.[12] According to this theory, the attachment rate coefficient is dependent on the mass transfer of colloids to the collector surface and subsequent colloid−surface interactions. CFT allows decoupling of surface energetics from system hydrodynamics by expressing the deposition rate coefficient in terms of the single collector efficiency (η) and the collision efficiency (α). The parameter η accounts for the mass flux of colloids to the collector surface and is defined as the ratio of the rate at which colloids strike the collector surface (r_s) to the rate at which particles flow toward the collector (r_f)[12] (i.e., $\eta = r_s/r_f$). The parameter η has been extensively studied for ideal systems composed of a spherical collector with a smooth surface. Correlation equations for calculating η as a function of parameters such as Peclet number, grain and colloid size, and colloid density have been presented.[13,14] More recently, the sensitivity of η to variations in collector shape and roughness was found to be significant.[15] The parameter α accounts for colloid−surface interactions, and is defined as the rate at which colloids collide with the collector surface and are successful in producing attachment (r_a) divided by the rate at which colloids strike the collector[12] (i.e., $\alpha = r_a/r_s$).

CFT assumes that colloids are irreversibly retained in the primary minimum of the Derjaguin−Landau−Verwey−Overbeek (DLVO) interaction energy profile.[16] In this case, physicochemical forces between colloids and collectors will determine the extent of attachment and the value of α.[16] These physicochemical forces include the electric double layer and London−van der Waals forces that are considered in the DLVO theory,[17,18]

* Corresponding author. Phone: 951-369-4857. E-mail: sbradford@ussl.ars.usda.gov.

[†] University of California, Riverside.

[‡] U.S. Department of Agriculture.

(1) McDowell-Boyer, L. M.; Hunt, J. R.; Sitar, N. Particle transport through porous media. *Water Resour. Res.* **1986**, *22*, 1901−1921.

(2) Ryan, J. N.; Elimelech, M. Colloid mobilization and transport in groundwater. *Colloids Surf., A: Physicochem. Eng. Aspects* **1996**, *107*, 1−56.

(3) Khilar, K. C.; Fogler, H. S. In *Migration of Fines in Porous Media: Theory and Applications of Transport in Porous Media*; Kluwer Academic Publishing; Dordrecht, The Netherlands, 1998.

(4) Kretzschmar, R.; Borkovec, M.; Grolimund, D.; Elimelech, M. Mobile subsurface colloids and their role in contaminant transport. *Adv. Agron.* **1999**, *66*, 121−193.

(5) Murphy, E. M.; Ginn, T. R. Modeling microbial processes in porous media. *Hydrogeol. J.* **2000**, *8* (1), 142−158.

(6) Schijven, J. F.; Hassanizadeh, S. M. Removal of viruses by soil passage: Overview of modelling, processes, and parameters. *Crit. Rev. Environ. Sci. Technol.* **2000**, *30*, 49−127.

(7) Jin, Y.; Flury, M. Fate and transport of viruses in porous media. *Adv. Agron.* **2002**, *77*, 39−102.

(8) Ginn, T. R.; Wood, B. D.; Nelson, K. E.; Schiebe, T. D.; Murphy, E. M.; Clement, T. P. Processes in microbial transport in the natural subsurface. *Adv. Water Res.* **2002**, *25*, 1017−1042.

(9) Rockhold, M. L.; Yarwood, R. R.; Selker, J. S. Coupled microbial and transport processes in soils. *Vadose Zone J.* **2004**, *3*, 368−383.

(10) Tufenkji, N. Application of a dual deposition mode model to evaluate transport of *Escherichia coli* D21 in porous media. *Water Resour. Res.* **2006**, *42*, Art. No. W12S11, doi:10.1029/2005WR004851.

(11) McCarthy, J. F.; Zachara, J. M. Subsurface transport of contaminants. *Environ. Sci. Technol.* **1989**, *26*, 496−502.

(12) Yao, K. M.; Habibian, M. T.; O'Melia, C. R. Water and waste water filtration − concepts and applications. *Environ. Sci. Technol.* **1971**, *5*, 1105−1112.

(13) Rajagopalan, R.; Tien, C. Trajectory analysis of deep-bed filtration with the sphere-in-cell porous media model. *AIChE J.* **1976**, *22* (3), 523−533.

(14) Tufenkji, N.; Elimelech., M. Correlation equation for predicting single-collector efficiency in physiochemical filtration in saturated porous media. *Environ. Sci. Technol.* **2004**, *38*, 529−536.

(15) Saiers, J. E.; Ryan, J. N. Colloid deposition on non-ideal porous media: The influences of collector shape and roughness on the single-collector efficiency. *Geophys. Res. Lett.* **2005**, *32*, Art. No. L21406, doi: 10.1029/2005GL024343.

(16) Elimelech, M.; Gregory, J.; Jia, X.; Williams, R. A. *Particle Deposition and Aggregation: Measurement, Modelling, and Simulation*; Butterworth-Heinemann: Oxford, England, 1995.

(17) Derjaguin, B. V.; Landau, L. D. Theory of the stability of strongly charged lyophobic sols and of the adhesion of strongly charged particles in solutions of electrolytes. *Acta Physicochim. USSR* **1941**, *14*, 733−762.

10.1021/la700995e CCC: $37.00
Published on Web 08/18/2007

as well as poorly characterized "non-DLVO" forces.[2] Therefore, the value of α should be controlled by the chemistry of the solid surface (mineralogy and organic matter content) and solution (pH and ionic strength). In homogeneous porous media, the value of α is equal to 1 under chemically favorable attachment conditions. In chemically heterogeneous porous media with localized regions that are favorable for attachment, the value of α is proportional to the fraction of the solid surface area that is "chemically favorable" for attachment.[19,20] Values of α have typically been determined from CFT using fitted values of the attachment coefficient obtained from experimental breakthrough curves and values of η estimated from published correlation expressions.[21,22] Alternatively, the value of α has been determined as the ratio of experimental deposition rate coefficients in "chemically unfavorable" to "chemically favorable" (colloids that strike the collector will all be attached) conditions.[23,24] Theoretical approaches for determining α have also been developed on the basis of the interaction force boundary layer (IFBL) approximation[2] and from the calculated probability of colloids escaping the secondary minimum of the DLVO interaction energy distribution by diffusion.[25,26] It should be noted that the aforementioned methods for determining α are based upon the assumption that α is independent of the flow characteristics of the system.

Under chemically favorable attachment conditions, it may be reasonable to assume that hydrodynamic forces will have a negligible effect on the value of α because of the very large adhesive force acting on colloids attached in the primary minimum that prevents particle release. However, a growing body of evidence suggests that attachment in the (chemically unfavorable) secondary minimum can significantly contribute to the retention of colloids in saturated porous media.[22−24,27−32] Notably, the assumption that hydrodynamic forces will not impact α is likely to be invalid when colloids are weakly attached in the secondary energy minimum. This has important implications for the determination of α under chemically unfavorable conditions. Indeed, recent experimental evidence demonstrates that the value of α decreases with increasing water velocity under unfavorable attachment conditions,[33−35] and colloids captured in the secondary energy minimum can be translated along the collector surface via hydrodynamic forces.[36]

Several researchers have studied the influence of hydrodynamic drag force on the detachment of particles attached in the primary minimum.[37−40] For example, Bergendahl and Grasso[40] demonstrated how polystyrene colloids that were attached (in the primary minimum) to glass beads in a packed column could be detached via hydrodynamic drag force at a pore water velocity of 157−630 m/day depending on the magnitude of the DLVO interaction forces. Such high velocities and hydrodynamic drag forces are, however, unlikely to occur in groundwater environments. In contrast, the influence of hydrodynamic shear on the attachment and detachment of particles in the secondary energy minimum has received little attention in the literature.[41] Colloids in the secondary minimum are expected to be much more sensitive to hydrodynamic shear than colloids in the primary minimum because of their weak association with the solid phase. The strength of this interaction is also a strong function of the solution chemistry, that is, the depth of the secondary energy minimum. Hence, attachment of colloids in the secondary minimum is anticipated to be a strong function of both hydrodynamics and solution chemistry. Therefore, on the basis of the depth of the secondary energy minimum and the distribution of hydrodynamic shear forces along the collector surface, it is possible that only a fraction of the collector surface area will contribute to attachment and, hence, to the determination of α.

The objective of this study is to quantify the influence of hydrodynamic and DLVO forces that act on attached colloids, and to determine the fraction of the single collector surface area that is "chemically and hydrodynamically favorable" for attachment. This was done by determining the fluid flow field around a single collector and calculating the DLVO and hydrodynamic forces and torques that act on attached colloids around the collector surface. Chemically and hydrodynamically favorable attachment areas on the collector surface were found to occur when the resisting torque due to DLVO forces was greater than the applied hydrodynamic torque. Moreover, the effect of colloid size as well as collector size and shape were evaluated in these calculations.

(18) Verwey, E. J. W.; Overbeek, J. T. G. *Theory of the Stability of Lyophobic Colloids*; Elsevier: Amsterdam, 1948.

(19) Elimelech, M.; Nagai, M.; Ko, C. H.; Ryan, J. N. Relative insignificance of mineral grain zeta potential to colloid transport in geochemically heterogeneous porous media. *Environ. Sci. Technol.* **2000**, *34*, 2143−2148.

(20) Abudalo, R. A.; Bogatsu, Y. G.; Ryan, J. N.; Harvey, R. W.; Metge, D. W.; Elimelech, M. Effect of ferric oxyhydroxide grain coatings on the transport of bacteriophage PRD1 and *Cryptosporidium parvum* oocysts in saturated porous media. *Environ. Sci. Technol.* **2005**, *39*, 6412−6419.

(21) Bales, R. C.; Hinkle, S. R.; Kroeger, T. W.; Stocking, K.; Gerba, C. P. Bacteriophage adsorption during transport through porous media: Chemical, perturbation and reversibility. *Environ. Sci. Technol.* **1991**, *25*, 2088−2095.

(22) Redman, J. A.; Walker, S. L.; Elimelech, M. Bacterial adhesion and transport in porous media: Role of the secondary energy minimum. *Environ. Sci. Technol.* **2004**, *38*, 1777−1785.

(23) Walker, S. L.; Redman, J. A.; Elimelech, M. Role of cell surface lipopolysaccharides in *Escherichia coli* K12 adhesion and transport. *Langmuir* **2004**, *20*, 7736−7746.

(24) Tufenkji, N.; Elimelech, M. Deviation from the classical colloid filtration theory in the presence of repulsive DLVO interactions. *Langmuir* **2004**, *20*, 10818−10828.

(25) Simoni, S. F.; Harms, H.; Bosma, T. N. P.; Zehnder, A. J. B. Population heterogeneity affects transport of bacteria through sand columns at low flow rates. *Environ. Sci. Technol.* **1998**, *32*, 2100−2105.

(26) Dong, H. Significance of electrophoretic mobility distribution to bacterial transport in granular porous media. *J. Microbiol. Methods* **2002**, *51*, 83−93.

(27) Franchi, A.; O'Melia, C. R. Effects of natural organic matter and solution chemistry on the deposition and reentrainment of colloids in porous media. *Environ. Sci. Technol.* **2003**, *37*, 1122−1129.

(28) Hahn, M. W.; O'Melia, C. R. Deposition and reentrainment of Brownian particles in porous media under unfavorable chemical conditions: Some concepts and applications. *Environ. Sci. Technol.* **2004**, *38*, 210−220.

(29) Hahn, M. W.; Abadzic, D.; O'Melia, C. R. Aquasols: On the role of secondary minima. *Environ. Sci. Technol.* **2004**, *38*, 5915−5924.

(30) Cushing, R. S.; Lawler, D. F. Depth filtration: Fundamental investigation through three-dimensional trajectory analysis. *Environ. Sci. Technol.* **1998**, *32*, 3793−3801.

(31) Tufenkji, N.; Elimelech, M. Breakdown of colloid filtration theory: Role of the secondary energy minimum and surface charge heterogeneities. *Langmuir* **2005**, *21*, 841−852.

(32) Tong, M.; Johnson, W. P. Colloid population heterogeneity drives hyperexponential deviation from classic filtration theory. *Environ. Sci. Technol.* **2007**, *41* (2), 493−499.

(33) Tong, M.; Li, X.; Brow, C. N.; Johnson, W. P. Detachment-influenced transport of an adhesion-deficient bacterial strain within water-reactive porous media. *Environ. Sci. Technol.* **2005**, *39*, 2500−2508.

(34) Li, X.; Johnson, W. P. Nonmonotonic variations in deposition rate coefficients of microspheres in porous media under unfavorable deposition conditions. *Environ. Sci. Technol.* **2005**, *39*, 1658−1665.

(35) Johnson, W. P.; Li, X.; Yal, G. Colloid retention in porous media: Mechanistic confirmation of wedging and retention in zones of flow stagnation. *Environ. Sci. Technol.* **2007**, *41* (4), 1279−1287.

(36) Kuznar, Z. A.; Elimelech, M. Direct microscopic observation of particle deposition in porous media: Role of the secondary energy minimum. *Colloids Surf., A: Physicochem. Eng. Aspects* **2007**, *294*, 156−162.

(37) Cleaver, J. W.; Yates, B. Mechanism of detachment of colloid particles from a flat substrate in turbulent flow. *J. Colloid Interface Sci.* **1973**, *44*, 464−474.

(38) Hubbe, M. A. Detachment of colloidal hydrous oxide spheres from flat surfaces exposed to flow. 1. Experimental system. *Colloids Surf.* **1985**, *16*, 227−248.

(39) Sharma, M. M.; Chamoun, H.; Sita Rama Sarma, D. S. H.; Schechter, R. S. Factors controlling the hydrodynamic detachment of particles from surfaces. *J. Colloid Interface Sci.* **1992**, *149* (1), 121−134.

(40) Bergendahl, J.; Grasso, D. Prediction of colloid detachment in a model porous media: Hydrodynamics. *Chem. Eng. Sci.* **2000**, *55*, 1523−1532.

(41) Bradford, S. A.; Torkzaban, S.; Walker, S. L. Coupling of physical and chemical mechanisms of colloid straining in saturated porous media. *Water Res.* **2007**, *41* (13), 3012−3024.

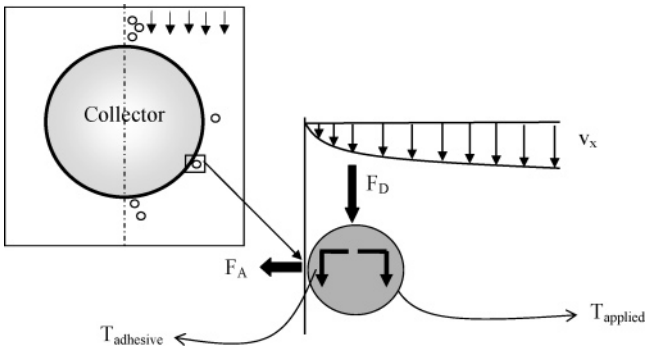

Figure 1. Schematic of colloid transport and attachment around a spherical collector according to the sphere-in-cell model. The applied torque acting on a colloid in the vicinity of the collector surface, $T_{applied}$, is caused by the drag force, F_D. The adhesive torque, $T_{adhesive}$, is caused by the adhesive (DLVO) force, F_A.

2. Methods

2.1. Modeling Approach. Various forces are exerted on attached colloids on the collector surface in a flow field. These forces include van der Waals forces, electrostatic double layer forces, and hydrodynamic forces.[2] The magnitudes of these forces are dependent on the physicochemical and hydrodynamic conditions of the system. Moreover, hydrodynamic forces (drag and lift) vary along the surface of the collector and are a function of the collector shape and size. A schematic of the forces and torques that act on attached colloids is presented in Figure 1. Fluid flow around the collector results in lift (F_L, MLT^{-2}, where M, L, and T denote units of mass, length, and time, respectively) and drag (F_D, MLT^{-2}) forces that act on attached colloids. The hydrodynamic shear that acts on the colloid surface facing the collector is different from that acting on the outer surface of the colloid surface facing the bulk fluid. This difference in shear force creates an applied moment or torque that acts on the attached colloid.[30] Adhesive physicochemical forces (F_A, MLT^{-2}) that serve to attach the colloids to the collector surface subsequently create a resisting torque against detachment in the presence of applied hydrodynamic forces. Through the summation of the calculated applied (hydrodynamic) and resisting (adhesive) torques that act on attached colloids, the fraction of the collector surface on which attachment may occur was determined.

Packed beds of granular media have been represented by many different configurations, including the sphere-in-cell model,[42,43] capillary tubes,[44] and constricted tubes.[40,45] In analogy to CFT, the sphere-in-cell model was adopted (Figure 1) in this work. The fluid cell dimensions were computed so that the porosity of the porous medium was preserved for the single collector. To compute the hydrodynamic forces acting on attached colloids, the fluid velocity field around the collector must be known. The Navier−Stokes equation in an axisymmetrical coordinate system was solved using the COMSOL software package (COMSOL, Inc., Palo Alto, CA) to determine the fluid velocity field around the collector surface. The mesh size was refined sufficiently near the collector surface (submicron to micron size) to yield the fluid velocity at the center of the colloid in the vicinity of the collector. A no-slip boundary condition was imposed along the collector surface, and the normal velocity and tangential stress at the side boundaries of the cell around the collector were set equal to zero. To reflect typical groundwater conditions, the simulations were performed with an average pore water velocity ranging from 0.1 to 60 m/day. A fixed pressure difference between the inlet and outlet boundary of the cell was imposed in order to achieve the desired average pore water velocities.

Three different colloid sizes with diameters of 0.5, 1, and 5 μm were employed. Colloids were assumed to be polystyrene latex microspheres with a density equal to water, such that the influence of gravity was neglected. Initial simulations discussed herein considered the influence of hydrodynamics and adhesive forces on the attachment of 0.5, 1, and 5 μm colloids onto a 400 μm diameter glass bead spherical collector. Additional simulations examined the attachment of 1 μm colloids at various ionic strengths to spherical glass bead collectors with diameters of 100, 200, 600, and 1000 μm at a constant pore water velocity of 3 m day^{-1}. In this case, the dimension of the cell around the collector was increased with the collector size so as to obtain the same average pore water velocity for the various collector sizes. Finally, other simulations were conducted to examine the attachment of 1 μm colloids at various ionic strengths to different shaped glass bead collectors at a constant pore water velocity of 1.5 m day^{-1}. In this latter case, three spheroidal collectors were considered, namely, spherical, oblate, and prolate. The aspect ratio (A_r), defined as the ratio of the lengths of the semiaxes oriented parallel and perpendicular to the flow directions, for spherical, oblate, and prolate spheroids was 1, 0.5, and 1.5, respectively, and the semiaxes oriented parallel to the flow direction were set equal to 400, 200, and 600 μm, respectively.

2.2. Calculation of Adhesive Force and Resisting Torque. DLVO theory[17,18] was applied to calculate the total interaction energy as the sum of van der Waals and electrostatic double layer interaction energies for 0.5, 1, and 5 μm colloids upon close approach to the collector surface for various solution chemistries (ionic strength (IS) ranged from 1 to 100 mM). The total interaction energy was determined by treating the colloid−collector system as a sphere−plate interaction. Electrostatic double layer interactions were determined using the constant surface potential interaction expression of Hogg et al.[46] with zeta potentials utilized in place of surface potentials. The retarded van der Waals interaction was determined using the expression by Gregory.[47] A value of 9.2×10^{-21} J was used for the Hamaker constant to be consistent with the assumed polystyrene microspheres−water−glass beads system.[48] Colloid and collector zeta potentials for various ionic strength conditions were assumed to be those reported by Kuznar and Elimelech[36] in a solution of pH 11, and ranged from −100 to −10 mV depending on the ionic strength.

To obtain the adhesive force that acts on attached colloids in terms of the calculated interaction energy, the Derjaguin and Langbein approximations[49] were employed. Specifically, the value of the adhesive force (F_A) was estimated as Φ_{min}/h, where Φ_{min} [ML^2T^{-2}] is the absolute value of the secondary or primary minimum interaction energy, and h [L] is the separation distance between the colloid and the solid surface.

The adhesive or resisting torque ($T_{adhesive}$, ML^2T^{-2}) for colloids attached in either the secondary or primary minimum was

(42) Happel, J. Viscous flow in multiparticle systems: Slow motion of fluids relative to beds of spherical particles. *AIChE J.* **1958**, *4*, 197−201.
(43) Payatakes, A. C.; Rajagopalan, R.; Tien, C. On the use of Happel's model for filtration studies. *J. Colloid Interface Sci.* **1974**, *49*, 321.
(44) Tien, C. *Granular Filtration of Aerosols and Hydrosols*; Butterworth-Heinemann Series in Chemical Engineering; Butterworth-Heinemann: Boston, MA, 1989.
(45) Payatakes, A. C.; Tien, C.; Turian, R. M. A new model for granular porous media. Part I. Model formulation. *AIChE J.* **1973**, *19*, 58.
(46) Hogg, R.; Healy, T. W.; Fuerstenau, D. W. Mutual coagulation of colloidal dispersions. *Trans. Faraday Soc.* **1966**, *62*, 1638−1651.
(47) Gregory, J. Approximate expression for retarded van der Waals interaction. *J. Colloid Interface Sci.* **1981**, *83*, 138−145.
(48) White, L. The theory of van der Waals forces. In *Foundations of Colloid Science*; Hunter, R. J., Ed.; Clarendon Press: Oxford, U.K., 1987; Vol. 1.
(49) Israelachvili, J. N. *Intermolecular and Surface Forces*, 2nd ed.; Academic Press: London, England, 1992.

represented by the net adhesive force (F_A) acting on a lever arm (l_x, L) as

$$T_{\text{adhesive}} = F_A l_x \quad (1)$$

The value of F_A corresponds to the DLVO force of adhesion which must be overcome in order to detach the particle from the secondary or primary energy minimum. The value of l_x is provided by the radius of the colloid−surface contact area that was estimated using the theory of Johnson, Kendall, and Roberts (1971)[50] known as the JKR theory. Since there is no direct physical contact between colloids attached in the secondary minimum and the collector, the corresponding contact radius is given as[49]

$$l_x = \left(\frac{F_A r_c}{4K}\right)^{1/3} \quad (2)$$

Here, r_c [L] is the colloid radius, and K is the composite Young's modulus.[50] Bergendahl and Grasso[40] employed a value of $K = 4.014 \times 10^9$ N m^{-2} for glass bead collectors and a polystyrene colloid suspension, and this value was assumed for the calculations discussed herein.

It should be mentioned that the JKR theory has been applied to investigate the influence of hydrodynamics on particle detachment under both favorable[40,51] and unfavorable[41] attachment conditions. It has been established in aquatic environments that colloids retained in the primary or secondary minimum do not have direct physical contact with the solid surface. This finding is more obvious for colloids attached in the secondary minimum. For separations of a few nanometers or less, non-DLVO forces will often produce strong repulsive forces that prevent the formation of a physical contact for colloids in the primary minimum.[2,16] Indeed, experimental work confirms the existence of this water layer and minor separation distance, in that colloids in the primary minimum can be released simply by altering the solution chemistry (i.e., increase in pH or decrease in ionic strength).[2,22] Hence, the only differences between colloids attached in the secondary and primary minimum are the magnitude of the adhesive force and the separation distance. If we therefore accept that there is an adhesive lever arm acting on colloids held in the primary minimum,[40,51] then there should also be an adhesive lever arm for colloids attached in the secondary minimum.[41]

2.3. Determination of Hydrodynamic Force and the Applied Torque. Under laminar flow conditions, the lift and drag forces acting on attached colloids were determined using the following equations:[52−54]

$$F_L = \frac{81.2\mu r_c^{\,3}(\partial V/\partial r)^{1.5}}{\nu^{0.5}} \quad (3)$$

$$F_D = 10.205\pi\mu(\partial V/\partial r) r_c^{\,2} \quad (4)$$

where V [LT^{-1}] is the pore water velocity, $\partial V/\partial r$ [T^{-1}] is the hydrodynamic shear at a distance of r_c from the surface, μ [ML^{-1}T^{-1}] is the fluid absolute viscosity, and ν [L^{2}T^{-1}] is the fluid kinematic viscosity.

For attachment to occur, the adhesive force acting on the colloid in the vicinity of the surface must overcome the repulsive and hydrodynamic forces. Lifting, sliding, and rolling are the hydrodynamic mechanisms that can cause colloid removal from the collector.[40] Rolling has been reported to be the dominant mechanism of detachment under laminar flow conditions.[40,55,56] Rolling occurs when the adhesive torque (the resistance to rolling) is overcome by the applied torque (T_{applied}, ML^{2}T^{-2}) from hydrodynamic forces.[57] The applied torque acting on the colloid in the vicinity of the collector surface due to the hydrodynamic shear force is given as[39,53,54]

$$T_{\text{applied}} = 1.4 r_c F_D \quad (5)$$

Because of the increase in velocity with distance from the collector surface, the drag force effectively acts on the attached particle at a height of $1.4r_c$; thus, the drag force creates a torque by acting on a lever arm of $1.4r_c$.

3. Results and Discussion

3.1. DLVO Calculations and Drag Forces. DLVO interaction energy profiles for the 0.5, 1, and 5 μm polystyrene latex microsphere colloids upon approach to glass bead collector surfaces were determined over a range of ionic strengths (1−100 mM). No barrier to attachment in the primary minimum was found to exist in the highest ionic strength solution, (i.e., chemically favorable attachment conditions). In contrast, calculations revealed the presence of an energy barrier against attachment in the primary minima at ionic strengths ranging from 1 to 90 mM. The height of the energy barrier to attachment in the primary minimum ranged from 1500 to 10 $k_b T_k$ (where k_b and T_k are the Boltzmann constant and the temperature in degrees Kelvin, respectively) for the 1 and 90 mM solutions. Under these chemically unfavorable attachment conditions, the DLVO calculations predict that colloids can still interact with the solid phase because of the presence of secondary energy minima at separation distances greater than the location of the energy barrier. To emphasize the magnitude of the secondary energy minimum, representative DLVO interaction energy profiles generated for 1 μm colloids at three different ionic strengths (10, 50, and 100 mM) are plotted in Figure 2. It is worth noting that the depth of secondary energy minimum increased with the colloid size as a result of an enhancement in attractive van der Waals interactions (Figure 3).

To investigate the accuracy of the finite element calculations for the flow field, the numerical results were compared with the analytical solution[58] of Stokes fluid flow around a circular collector grain. Excellent agreement was obtained between the analytic and numerical results, demonstrating the ability of the finite element model to accurately simulate the velocity distribution around the collector. Figure 4 presents the calculated distribution of the tangential component of drag force that acts on the colloids (0.5, 1, and 5 μm) in the vicinity of the spherical collector when the pore water velocity is 3 m day^{-1}. The distribution of tangential drag force along the collector surface is plotted versus normalized distance ($L/L_{\max}$), which is defined as the distance from the front toward the rear stagnation point

(50) Johnson, K. L.; Kendall, K.; Roberts, A. D. Surface energy and the contact of elastic solids. *Proc. R. Soc. London, Ser. A* **1971**, *324*, 301−313.
(51) Bergendahl, J.; Grasso, D. Prediction of colloid detachment in a model porous media: Thermodynamics. *AIChE J.* **1999**, *45* (3), 475−484.
(52) Saffman, P. G. The lift on a small sphere in a slow shear flow. *J. Fluid Mech.* **1965**, *22*, 385−400.
(53) Goldman, A. J.; Cox, R. G.; Brenner, H. Slow viscous motion of a sphere parallel to a plane wall − I motion through a quiescent fluid. *Chem. Eng. Sci.* **1967**, *22*, 637−651.
(54) O'Neill, M. E. A sphere in contact with a plane wall in a slow linear shear flow. *Chem. Eng. Sci.* **1968**, *23*, 1293−1298.
(55) Tsai, C. J.; Pui, D. Y. H.; Liu, B. Y. H. Particle detachment from disk surfaces of computer disk drives. *J. Aerosol Sci.* **1991**, *22*, 737−746.
(56) Bergendahl, J.; Grasso, D. Colloid generation during batch leaching tests: Mechanics of disaggregation. *Colloids Surf., A: Physicochem. Eng. Aspects* **1998**, *135*, 193−205.
(57) Johnson, K. L. In *Contact Mechanics*, 1st ed.; Cambridge University Press: Cambridge, U.K., 1985.
(58) Bird, R. B.; Stewart, W. E.; Lightfoot, E. N. *Transport Phenomena*, 2nd ed.; J. Wiley and Sons: New York, 2002.

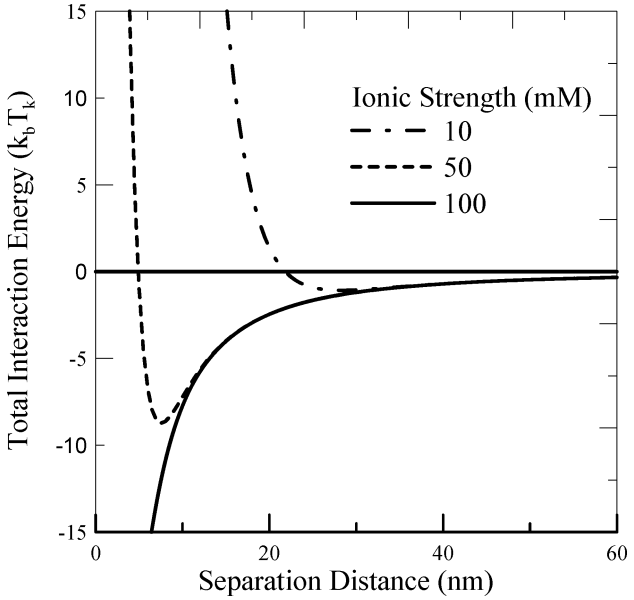

Figure 2. The total interaction energy as a function of separation distance between the 1 μm colloids and glass bead collector at several ionic strengths (10, 50, and 100 mM), emphasizing the secondary energy minimum.

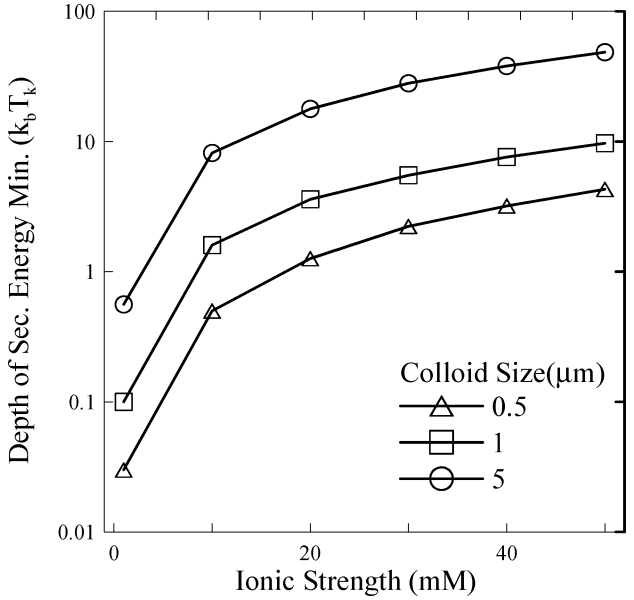

Figure 3. The depth of the secondary energy minimum as a function of ionic strength for three colloid sizes (0.5, 1.0, and 5 μm).

(L) divided by the distance between the front and rear stagnation points (L_{max}). The drag force was dependent on the location on the collector surface. The drag force was zero at the rear and forward stagnation points, and increased with the distance from these points until it reached a maximum value at the collector midpoint. As expected, larger colloids experienced greater drag forces at a given location on the collector surface.

3.2. Dependence of Attachment on the Interaction Energy and Fluid Velocity. Figure 5 shows a plot of the fraction of the spherical collector surface area that is "chemically and hydrodynamically favorable" for attachment (S_f) as a function of the average pore water velocity and the adhesive force for 1 μm colloids. Values of F_A in Figure 5 cover the range that may occur for glass bead and polystyrene colloids (F_A ranged from 1×10^{-9} to 1×10^{-14} N). The pore water velocity ranged from 0.1 to 60 m day^{-1}, which encompasses the realm of typical groundwater velocities. The value of S_f was a function of both

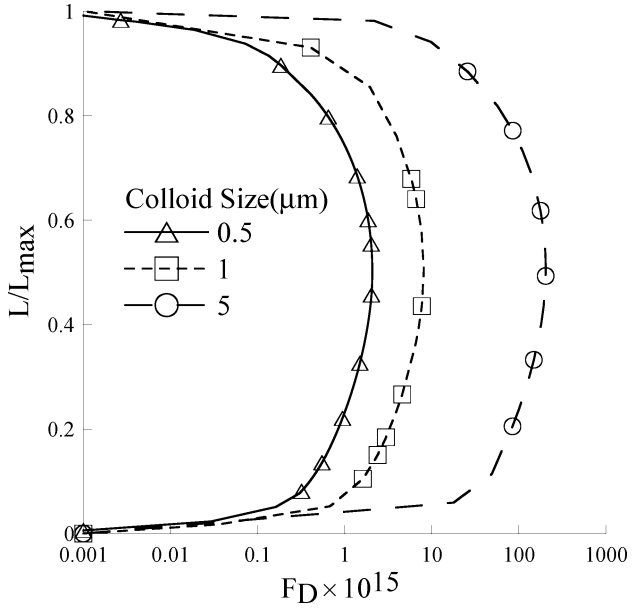

Figure 4. The calculated distribution of the tangential component of drag force that acts on the colloids (0.5, 1, and 5 μm) in the vicinity of the 400 μm spherical collector when the pore water velocity is 3 m day^{-1}. The distribution of tangential drag force along the collector surface is plotted versus normalized distance (L/L_{max}), which is defined as the distance from the front toward the rear stagnation point (L) divided by the distance between the front and rear stagnation points (L_{max}).

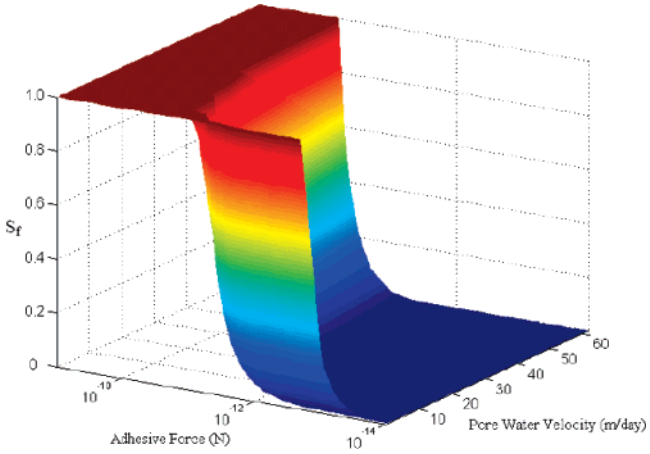

Figure 5. A plot of the fraction of the spherical collector surface area that is "chemically and hydrodynamically favorable" for attachment (S_f) as a function of the average pore water velocity and the adhesive force for 1 μm colloids.

F_A and the pore water velocity. The value of S_f decreased with decreasing F_A and increasing pore water velocity.

Figure 6 presents plots of S_f as a function of the pore water velocity at several ionic strengths (40, 60, 80, and 100 mM) for 0.5 (Figure 6a), 1 (Figure 6b), and 5 (Figure 6c) μm colloids. These plots can be discussed in terms of "favorable", "partially favorable", and "unfavorable" attachment conditions when considering both chemical and hydrodynamic forces. "Favorable" attachment conditions exist when $T_{adhesion} > T_{applied}$ over the entire collector surface and the value of $S_f = 1$. At an ionic strength of 100 mM, the DLVO calculations showed the existence of a primary minimum where no barrier to colloid deposition existed (Figure 2); hence, colloid attachment was hydrodynamically and chemically favorable over the entire collector grain for all the velocities considered (Figure 6). This result indicates that hydrodynamic forces probably have a negligible effect on the

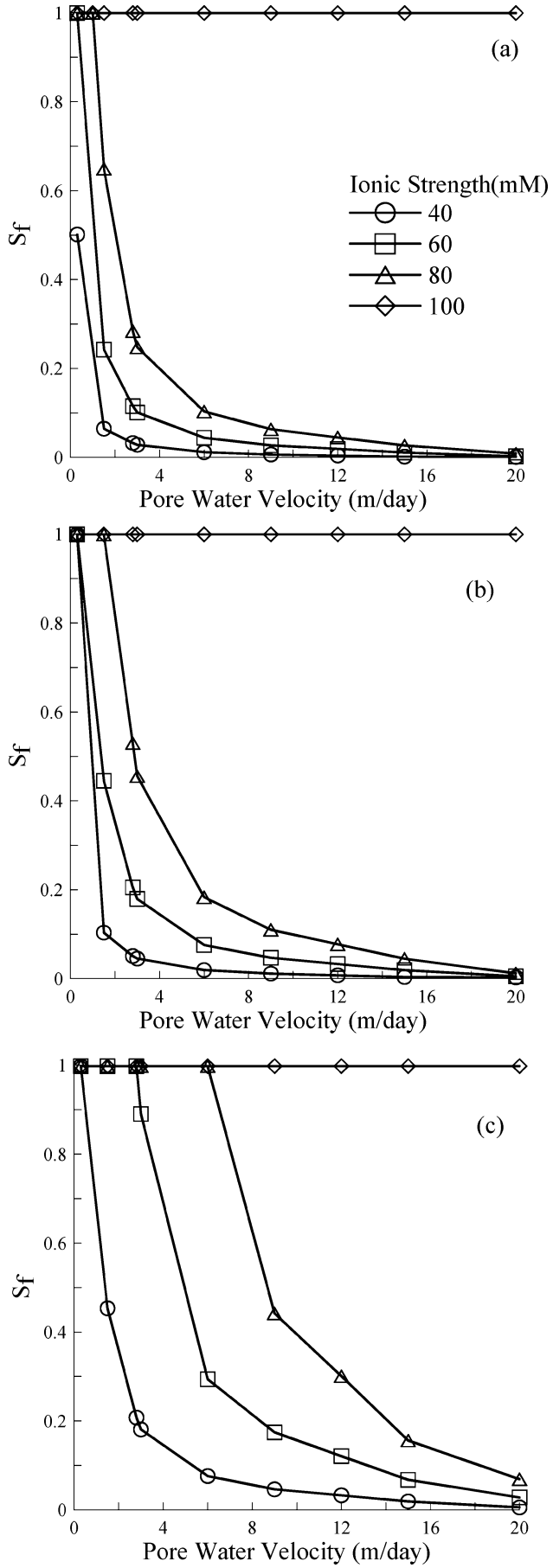

Figure 6. A plot of S_f as a function of the pore water velocity at several ionic strengths (40, 60, 80, and 100 mM) for 0.5 (a), 1 (b), and 5 μm (c) colloids.

collision efficiency under chemically favorable conditions. Notice that "favorable" attachment conditions ($S_f = 1$) may also exist at low pore water velocities because of the presence of the secondary minimum. Recall that the depth of the secondary minimum and $T_{adhesion}$ increased with ionic strength and colloid size (Figure 3). Hence, for a given colloid size and ionic strength there was a critical velocity at which the adhesive and applied torques were equal (i.e., $T_{adhesion} = T_{applied}$), and velocities that were lower than this critical value yielded $T_{adhesion} > T_{applied}$ and $S_f = 1$.

"Unfavorable" attachment conditions exist when $T_{adhesion} < T_{applied}$ occurs over the vast majority of the collector surface, and the value of S_f therefore approaches zero. In Figure 6, this happened above a pore water velocity of around 20 m day^{-1} for the 40, 60, and 80 mM conditions. As the pore water velocity decreased, however, the value of S_f increased and was between 0 and 1. This situation is referred to as "partially favorable" attachment conditions. In this portion of the plot, the collector surface exhibited regions that were "favorable" ($T_{adhesion} \geq T_{applied}$) and others that were "unfavorable" ($T_{adhesion} < T_{applied}$) for attachment. Figure 4 shows that the drag forces are lowest near the front and rear stagnation points of the collector, and highest near the collector center. The regions near the front and rear stagnation points are therefore the first to become "favorable" for attachment with decreasing pore water velocity or increasing ionic strength. Conversely, the collector center is the last region to become "favorable" for attachment. For a given colloid size, the velocity at which S_f rapidly decreased depended on the ionic strength. At a higher ionic strength, the rapid decrease in S_f occurred at a larger velocity due to the greater value of $T_{adhesion}$. Similarly at a given ionic strength, larger colloids exhibited a rapid decrease in S_f at a higher velocity than the smaller colloids. This observation can be attributed to the higher value of adhesive force (Figure 3) and lever arm for the larger colloids, which compensated for the higher drag force acting on the larger colloids (Figure 4).

Figure 7 presents similar information to Figure 6. In this case, however, plots of S_f are given as a function of ionic strength at several pore water velocities (0.3, 1.5, 6, and 12 m day^{-1}). For a given pore water velocity, colloid deposition increased with ionic strength. At low ionic strengths that are typical of most groundwater conditions (IS < 20 mM), the value of S_f was generally very low, and little attachment was possible on the collector surface. Under these "unfavorable" attachment conditions, a shallow secondary minimum existed at a relatively large distance from the surface of the collector, and colloids that collided with the collector were swept away by hydrodynamic shear ($T_{adhesion} < T_{applied}$). As the ionic strength of the solution increased, the depth of secondary minimum increased (Figure 2) and "partially favorable" attachment conditions occurred. In this case, S_f values varied between 0 and 1 because locations adjacent to the front and rear stagnation points became "favorable" for attachment ($T_{adhesion} > T_{applied}$), whereas regions adjacent to the collector center were still "unfavorable" for attachment ($T_{adhesion} < T_{applied}$). As the ionic strength continued to increase, "favorable" attachment conditions eventually existed over the entire collector surface. As in Figure 6, the shape of the plots shown in Figure 7 was highly dependent on the pore water velocity and the colloid size. For a given colloid size, increasing the pore water velocity increased $T_{applied}$ and therefore tended to push the plots shown in Figure 7 to the right (i.e., small values of S_f). The larger colloids, however, exhibited a decreased sensitivity to changes in velocity compared to that of the smaller colloids because they

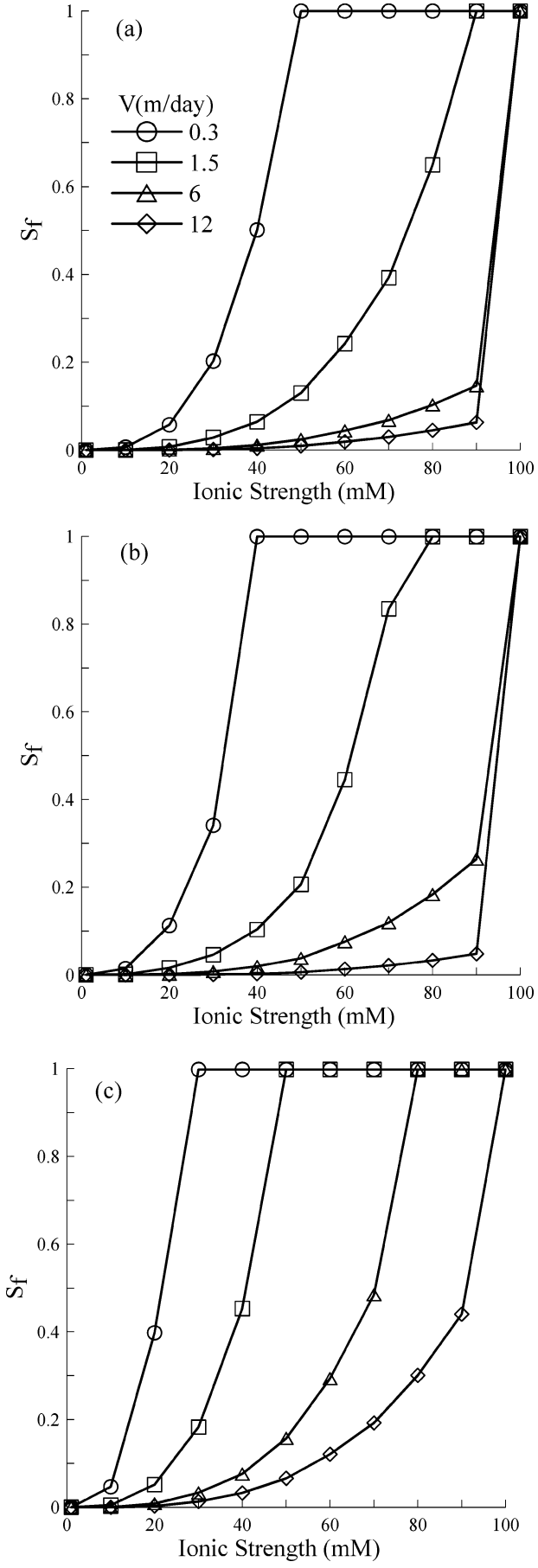

Figure 7. A plot of S_f as a function of ionic strength at several pore water velocities (0.3, 1.5, 6, and 12 m day^{-1}) for 0.5 (a), 1 (b), and 5 μm (c) colloids.

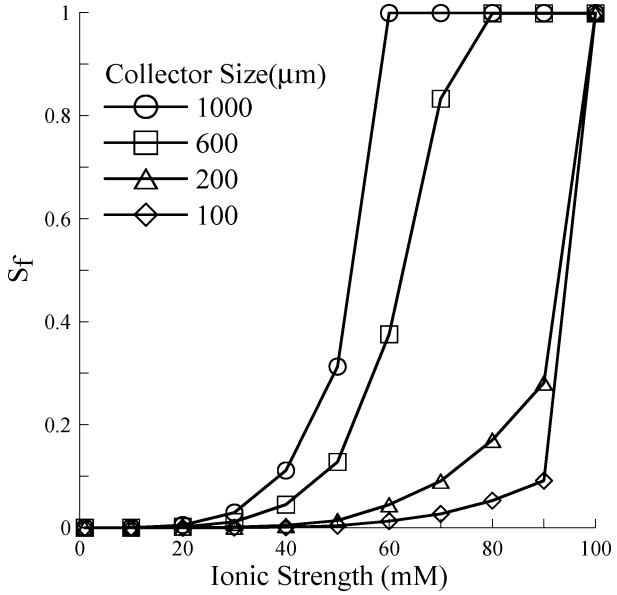

Figure 8. A plot of S_f for 1 μm colloids as a function of ionic strength for various spherical collector sizes (100, 200, 600, and 1000 μm) when the average pore water velocity was 3 m day^{-1}.

were associated with larger values of adhesive force (Figure 3) and lever arm at a given ionic strength.

3.3. Dependence of Attachment on Collector Size. Figure 8 presents an illustrative plot of S_f for 1 μm colloids as a function of ionic strength for various spherical collector sizes (100, 200, 600, and 1000 μm) when the average pore water velocity was 3 m day^{-1}. The value of $T_{adhesion}$ was the same for the various collectors at a given ionic strength. Hence, differences in Figure 8 occurred as a result of changes in $T_{applied}$ acting on the colloids that were in the vicinity of the different sized collectors. Figure 9 presents the calculated distribution of the tangential component of drag force that was exerted on the colloids in the vicinity of the collectors at this water velocity with normalized distance along the collector surface. The drag force that acted on the colloids along the collector surface decreased with increasing collector size. A simple verification of this finding is obtained by calculating the average Stokes drag force (on the collector surface) per unit surface area of the collector, which is equal to $3\mu V/D_c$ (where D_c [L] is the diameter of the collector) and predicts an inverse relationship with the collector diameter.

With these differences in mind, it is easier to interpret Figure 8. At lower ionic strengths, the value of S_f is controlled by "favorable" attachment conditions near the front and rear stagnation points. In these regions, the drag forces were similar in magnitude for the different sized collectors (Figure 9), and the value of S_f was therefore similar for the various collector sizes. Conversely, as the ionic strength increased, the value of S_f was controlled by the "unfavorable" attachment locations adjacent to the collector center. Since the larger collectors had lower drag forces in these locations (Figure 9), they also had the highest values of S_f. Conversely, higher values of S_f for smaller collectors were only possible at higher ionic strengths that approached chemically favorable attachment conditions in the primary minimum. This analysis predicts that larger collectors will have greater amounts of attachment than smaller collectors under chemically unfavorable conditions. This result is somewhat surprising since smaller collectors are frequently reported to be associated with greater amounts of colloid retention.[41,59] These findings may be explained by considerations of the pore structure and surface roughness that are neglected in CFT.[60] Additional

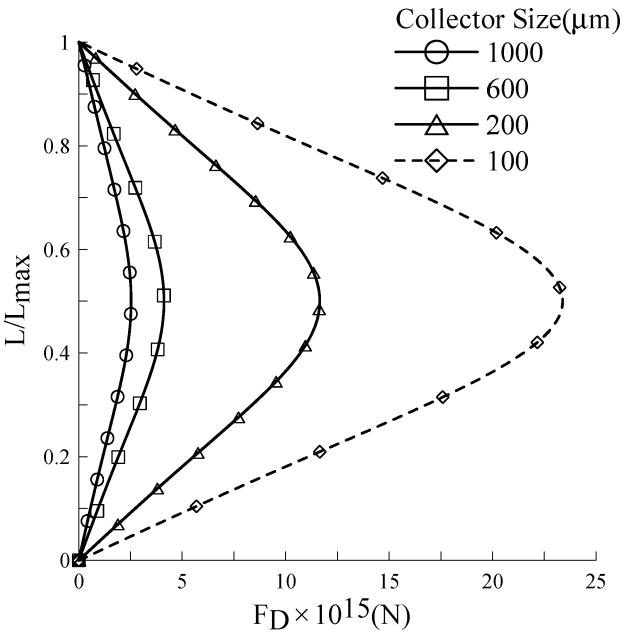

Figure 9. The calculated distribution of the tangential component of drag force that acts on 1 mm colloids in the vicinity of 100, 200, 600, and 1000 μm spherical collectors when the pore water velocity is 3 m day^{-1}. The distribution of the tangential component of drag force along the collector surface is plotted versus normalized distance (L/L_{max}), which is defined as the distance from the front toward the rear stagnation point (L) divided by the distance between the front and rear stagnation points (L_{max}).

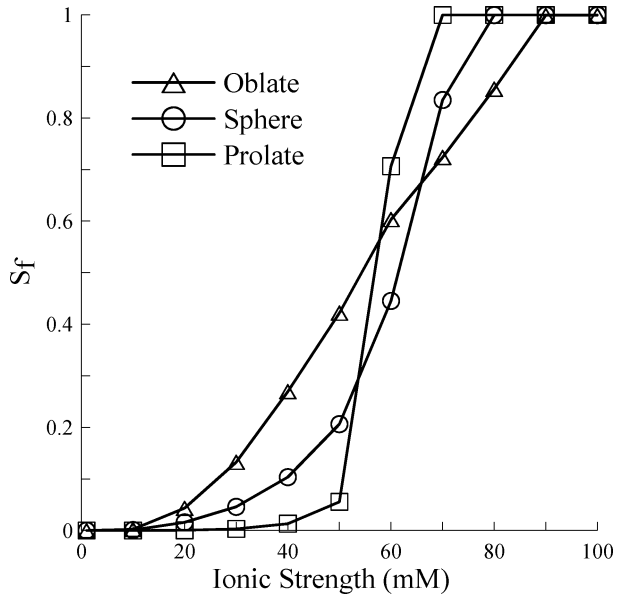

Figure 10. A plot of S_f as a function of ionic strength for 1 μm colloids in the vicinity of variously shaped spheroids (spherical, oblate, and prolate) in the presence of an average pore water velocity of 1.5 m day^{-1}.

research is warranted to prove this hypothesis, but is beyond the scope of this work.

3.4. Dependence of Attachment on Collector Shape. Figure 10 presents an illustrative plot of S_f as a function of ionic strength for 1 μm colloids that are attached to variously shaped spheroids (spherical, oblate, and prolate) in the presence of an average pore water velocity of 1.5 m day^{-1}. Similar to Figure 8, the value of $T_{adhesion}$ is the same for the various spheroids at a given ionic strength, and differences in Figure 10 therefore occur as a result of changes in $T_{applied}$. The lowest drag force occurred on the collector surface near the front and rear stagnation points, and these regions were larger for the oblate spheroid, followed by the sphere and then the prolate spheroid. Conversely, near the collector center, the drag force was lowest for the prolate spheroid, followed by the sphere, and then the oblate spheroid. At lower ionic strengths, the value of S_f in Figure 10 was controlled by "favorable" attachment regions near the front and rear stagnation points. Hence, oblate spheroids exhibit the highest values of S_f, followed by the sphere, and then the prolate spheroid. Conversely, at the higher ionic strengths, the value of S_f in Figure 10 was controlled by the "unfavorable" attachment locations adjacent to the collector center. Hence, prolate spheroids had the highest values of S_f, followed by the sphere, and then the oblate spheroid.

4. Summary and Conclusions

The goal of this research was to quantify the influence of the hydrodynamic and adhesion forces that act on colloids in the vicinity of the collector surface, and to determine the fraction of the single collector surface area that is available for attachment. This was done by solving the fluid flow field around a single collector, and then calculating the adhesion and hydrodynamic forces and torques that act on attached colloids. Three conditions were identified in these simulations when considering both chemical and hydrodynamic forces on attachment. "Favorable" attachment conditions occurred when the adhesive torque was greater than the applied hydrodynamic torque over the entire collector surface area, and, in this case, $\alpha = 1$. "Unfavorable" attachment conditions occurred when the adhesive torque was less than the applied hydrodynamic torque over the vast majority of the collector surface, and α was therefore close to 0. Finally, "partially favorable" attachment conditions occurred on a collector when the adhesive torque was greater than the applied hydrodynamic torque near the front and rear stagnation points, but was less than this applied torque near the collector center. "Partially favorable" attachment conditions exist when colloids are weakly associated with the solid phase via the secondary minimum, and the simulation results indicated that this condition can commonly exist under many physically relevant scenarios that are encountered in natural environments. "Partially favorable" conditions were found to be a strong function of the solution ionic strength, the zeta potential of the colloid and the collector surfaces, the pore water velocity, the colloid size, and the size and shape of the collector.

The determination of α under "partially favorable" attachment conditions is much more complex than that for "favorable" conditions. Under "partially favorable" conditions, the value of α is expected to be proportional to S_f. Additional complications may arise, however, because colloids that collide with the collector in "unfavorable" regions near the collector center may translate along the collector surface until they reach "favorable" attachment regions that are located adjacent to the rear stagnation point. Hence, it is possible that a fraction of the colloids that collide with "unfavorable" regions of the collector surface may also contribute to the determination of α. This is currently a topic of ongoing investigation, but is beyond the scope of this work.

Acknowledgment. This research was supported by the 206 Manure and Byproduct Utilization Project of the USDA-ARS and by a grant from the NRI (NRI # 2006-02541). Although this

(59) Bradford, S. A.; Yates, S. R.; Bettahar, M.; Simunek, J. Physical factors affecting the transport and fate of colloids in saturated porous media. *Water Resour. Res.* **2002**, *38* (12), Art. No. 1327, doi:10.1029/2002WR001340.

(60) Bradford, S. A.; Simunek, J.; Bettahar, M.; van Genuchten, M. Th.; Yates, S. R. Significance of straining in colloid deposition: Evidence and implications. *Water Resour. Res.* **2006**, *42*, Art. No. W12S15, doi:10.1029/2005WR004791.

work has been supported by the USDA, it has not been subjected to Agency review and therefore does not necessarily reflect the views of the Agency, and no official endorsement should be inferred. Similarly, mention of trade names and company names in this manuscript does not imply any endorsement or preferential treatment by the USDA.

LA700995E